

# Radiation and Diffraction Effects by Convex and Concave Domes\*

HIDEO SUZUKI\*\* AND JIRI TICHY

*Pennsylvania State University, Applied Research Laboratory, University Park, PA 16801, USA*

The effects of the diaphragm shape of a loudspeaker on the radiation characteristics are discussed using convex and concave domes in an infinite baffle. The results show that these characteristics are highly dependent on the shape of the diaphragm, even if it vibrates like a piston. The concave dome has a wide peak due to the cavity resonance resulting in higher radiation efficiency. The convex dome has lower on-axis pressure response in the same region due to the dispersion of energy to the off-axis direction. The diffraction of sound from a concentric ring source by the convex and concave domes is also investigated in order to discuss the interaction between the loudspeaker units of a complete system. The radiation and diffraction phenomena are well explained by the use of a graphic representation of the energy flow and pressure distributions.

## 0 INTRODUCTION

The cone-type loudspeaker has been used since the birth of the direct-radiator loudspeaker. The reason for this is the mechanical strength against the force given through the voice coil due to the diaphragm shape. A paper cone, because of its relatively large Young's modulus to density ratio  $E/\rho$  and high loss factor, has been used as the main loudspeaker diaphragm of the direct-radiator loudspeaker. But as long as paper is used as a diaphragm material,  $E/\rho$  does not have enough margin for us to try a flat or a very shallow diaphragm.

The situation has been changed, however, since composite materials with large  $E/\rho$  have come into use. With these materials it has become possible to try any kind of diaphragm shape, even the flat diaphragm. At this point we naturally come to the question, "What is the best shape as a radiator?" The diaphragm shape has effects on both the vibration and the radiation characteristics. These latter effects, however, have not had much attention paid to them up until now [1], [2]. Here we discuss the radiation and diffraction phenomena of convex and concave domes in an infinite baffle. This will give us a general idea about the differences in the radiation and diffraction effects of different kinds of diaphragm shapes.

\* Presented at the 67th Convention of the Audio Engineering Society, New York, 1980 October 31–November 3; revised 1981 January 16.

\*\* Now with CBS Technology Center, Stamford, CT 06905.

## 1 GEOMETRY OF THE MODEL

Fig. 1 shows a convex dome radiator with radius  $A$  and height  $H$  in an infinite baffle. The dome is represented as a portion of a sphere with radius  $R$ . It vibrates sinusoidally in the  $z$  direction with a constant velocity distribution of amplitude  $U_0$ . The assumption of this pistonlike motion may not be suitable in the high-frequency region because of the breakup of the diaphragm, but it will be beneficial for basic discussions of sound radiation and diffraction. Fig. 1 also shows a concentric circular line source with radius  $A_1$  (which will be called ring source hereafter) in an infinite baffle. For the radiation problem this ring source is neglected, and  $U_0$  is set equal to zero for the diffraction problem.

Fig. 2 shows a concave dome in an infinite baffle with a concentric ring source. The geometrical constants and velocity distributions are defined in a way similar to the case of the convex dome.

## 2 MATHEMATICAL METHOD

### 2.1 General Procedure

We will discuss briefly the method used in our radiation and diffraction problems. A more detailed discussion of the radiation from convex and concave domes in an infinite baffle is given in [3].

The wave equation in a space  $V$  filled with a fluid medium is expressed by the Helmholtz equation

$$\nabla^2 \psi(x) + k^2 \psi(x) = 0, \quad x \in V \tag{1}$$

where  $\nabla^2$  is the Laplacian operator,  $\psi(x)$  is the velocity potential,  $k$  is the wave number, and  $x$  is the field point. The pressure  $p(x)$  and the particle velocity  $u(x)$  are related to  $\psi(x)$  by

$$p(x) = j\omega\rho\psi(x) \tag{2}$$

$$u(x) = -\nabla\psi(x) \tag{3}$$

where  $\omega$  is the angular frequency,  $\rho$  is the density of the medium, and  $\nabla$  is the gradient operator.

The boundary condition on a surface  $S$  (which will be called the boundary surface) is generally expressed by

$$L\psi(x) = f(x), \quad x \in S. \tag{4}$$

The most common cases are the Dirichlet and Neumann boundary conditions expressed by

$$L = j\omega\rho \tag{5a}$$

$$f(x) = \text{prescribed pressure distribution} \tag{5b}$$

and

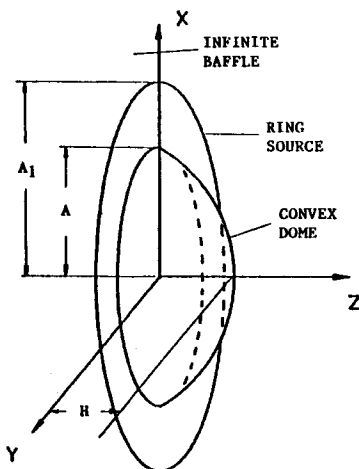


Fig. 1. Geometry of the convex dome with a ring source.

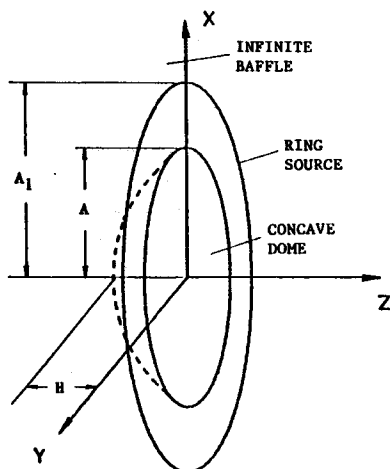


Fig. 2. Geometry of the concave dome with a ring source.

$$L = -\frac{\partial}{\partial n} \tag{6a}$$

$$f(x) = \text{prescribed velocity distribution} \tag{6b}$$

respectively.

Now the solution of Eq. (1) is expressed in the following form:

$$\psi(x) = \sum_{n=0}^{\infty} a_n \psi_n(x) \tag{7}$$

where  $a_n$  is the unknown coefficient and  $\psi_n(x)$  is the appropriate trial function that satisfies Eq. (1). When the above series is truncated at  $n = N$ , the boundary condition is satisfied only approximately. Then the "best approximation" may be defined as a solution of a set of unknown coefficients that makes the following error factor minimum [4]:

$$E = \int_S \left| \sum_{n=0}^N a_n L\psi_n(x) - f(x) \right|^2 dS. \tag{8}$$

Eq. 8 is the squared summation of the deviation of the approximated boundary value from the prescribed boundary value. From the condition that the set of  $a_n$ 's must make  $E$  minimum, we obtain the  $(N + 1)$  simultaneous equations [5]

$$\sum_{n=1}^N a_n \int_S \Psi_m^*(x) \Psi_n(x) dS = \int_S f(x) \Psi_m^*(x) dS \tag{9}$$

where

$$\Psi_n(x) = L\psi_n(x) \tag{10}$$

The solution of Eq. (9) determines the unknown coefficients  $a_n, n = 0, 1, \dots, N$ .

### 2.2 Radiation Problem

First the radiation from a convex dome will be discussed. For the convenience of the calculation, a model slightly different from Fig. 1 is used. The infinite baffle can be removed without any change of the sound field in the semi-infinite space on the right side if we assume that there exists a symmetric dome on the left side which is the mirror image of the dome on the right side (see Fig. 3). The velocity potential in the infinite space is expanded in the following form:

$$\psi(x) = \sum_{n=0}^{\infty} a_n h_n^{(2)}(kr) P_n(\cos \theta) \tag{11}$$

where  $h_n^{(2)}(kr)$  is the spherical Hankel function and  $P_n(\cos \theta)$  is the Legendre function with the polar coordinate system  $(r, \theta, \phi)$ . The boundary surface  $S$  is taken as the sphere with the origin  $O_1$  shown in Fig. 3. On the radiator surface the boundary condition is given by the Neumann boundary condition with  $L = -\partial/\partial n$  and  $f(x) = U_0 \cos \theta$ . On the imaginary surface  $S_2$  the condition of symmetry is used, that is, the potential at point

$P$  must be equal to the potential at point  $P_1$ . The operator  $L$  is interpreted as the one that gives the difference of the velocity potentials at the point of interest and its related point. Therefore

$$\Psi_n(x) = L\psi_n(x) = \psi_n(x) - \psi_n(x_1) \quad (12)$$

with  $f(x) = 0$ , where  $x_1$  is the symmetry point of  $x$ .

In the case of the concave dome the velocity potential inside the sphere is expressed by

$$\psi(x) = \sum_{n=0}^{\infty} a_n j_n(kr) P_n(\cos \theta) \quad (13)$$

where  $j_n(kr)$  is the spherical Bessel function. The boundary surface  $S$  consists of the radiator surface  $S_1$  and the opening of the cavity  $S_2$ . On the surface  $S_1$  the boundary condition is given by Eq. (6). On the surface  $S_2$  the normal velocity distribution is obtained (with unknown coefficients) by differentiating Eq. (13) with respect to  $z$ . Then, using the Rayleigh integral, the velocity potential on the opening  $S_2$  is obtained, which must be equal to Eq. (13). This results in an equation similar in form to Eq. (12). At this point the procedure is the same as in the case of the convex dome.

### 2.3 Diffraction Problem

The model shown in Fig. 3 is also applicable for the diffraction problem of the convex dome if we assume the existence of the ring source. The sound field in this case is expressed by

$$\psi_t(x) = \psi_s(x) + \psi_d(x) \quad (14)$$

where  $\psi_s(x)$  is the radiated sound field by a ring source, and  $\psi_d(x)$  is the diffracted sound field given by the form of Eq. (11). This velocity potential is obtained simply by replacing  $U_0 \cos \theta$  in the radiation problem by the normal velocity distribution on  $S_1$ , which is given by  $-(\partial/\partial n)(\psi_s)$ .

In the case of the concave dome the total velocity potential inside the sphere  $\psi_t(x)$ , which is expanded in

the same form as Eq. (13), must satisfy the Neumann boundary condition with  $U_0 = 0$ . Outside the cavity the total velocity potential is found by taking the Rayleigh integral of the normal velocity distribution on the baffle surface. Thus we have

$$\psi_t(x) = \psi_s(x) + \psi_n(x) \quad (15)$$

where  $\psi_s(x)$  is the velocity potential due to the ring source, and  $\psi_n(x)$  is the velocity potential obtained from the normal velocity distribution on the opening  $S_2$ , which can be expressed with unknown coefficients obtained from the total velocity potential  $\psi_t(x)$ . At this point the procedure is the same as in the radiation problem.

### 2.4 Geometrical Approximation

For the radiation problem, when we assume that an infinite number of point sources are distributed in such a way that they form the shape of the radiator with equal surface density in an infinite space, the on-axis sound pressure response is obtained by

$$P_0 = 2\{\exp[ikR(1 - \cos \theta_0)](ikR - 1) + (1 - \cos \theta_0 \cdot ikR)\}/\sin^2 \theta_0(ikR)^2 \quad (16)$$

The results will be compared with those obtained by the methods discussed above.

## 3 RESULTS AND DISCUSSIONS

### 3.1 Radiation from Convex and Concave Domes

#### 3.1.1 On-Axis Sound Pressure Response

Figs. 4 and 5 show on-axis sound pressure responses of convex and concave domes, respectively, along with those obtained by geometrical approximation. The response of the convex dome around  $kA = 1.0-2.0$ , which is within the range of reproduction of an actual dome-type loudspeaker, decreases as the height of the dome increases. As the results show, the dome-type loudspeaker with an  $H/A$  ratio of 0.6-0.8 has to suffer a decrease of response of about 3-7 dB, even if the diaphragm vibrates like a piston. It is not an unusual experience to see a "high-quality" dome-type loudspeaker with double humps at both ends of the reproducing range. Obviously the first hump is due to the fundamental resonance and the second is due to the breakup of the diaphragm. Between these humps the response goes down due to the radiation effect. This phenomenon should be kept in mind when designing a dome-type loudspeaker.

The concave dome, on the other hand, has a wide peak around  $kA = 1.0-1.5$  due to the resonance effect of the cavity (see Fig. 5). In the actual cone-type loudspeaker this phenomenon is not usually observed, because the frequency of the breakup of the cone falls mostly into this region. The fact that the responses of

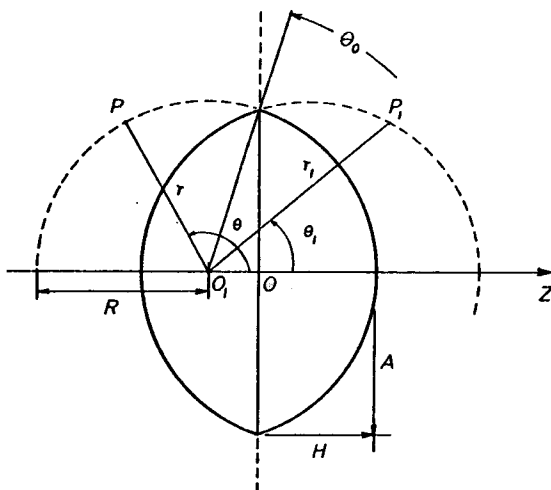


Fig. 3. Geometry of the convex dome radiator used for calculation.

the convex and concave domes are intrinsically different may mean that the sound quality of them may also have basic differences.

The results obtained by geometrical approximation are in good agreement with those of the convex dome in the high-frequency region ( $kA \geq 5.0$ ). These results

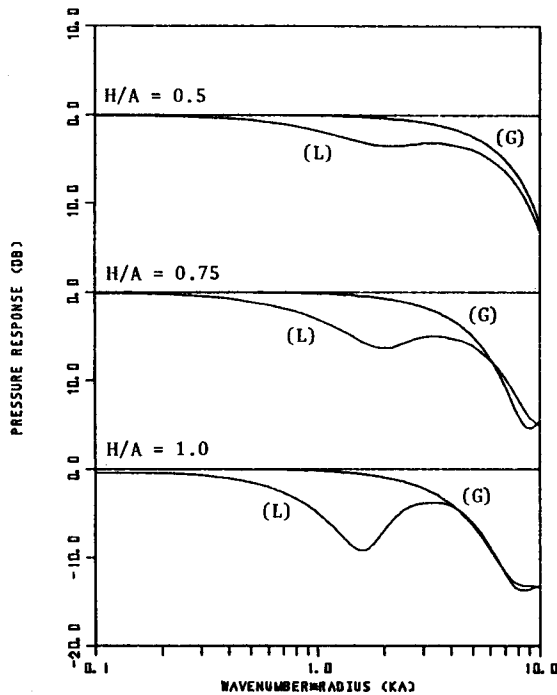


Fig. 4. On-axis pressure responses of a convex dome by the least-square error method (L) and by geometrical approximation (G).

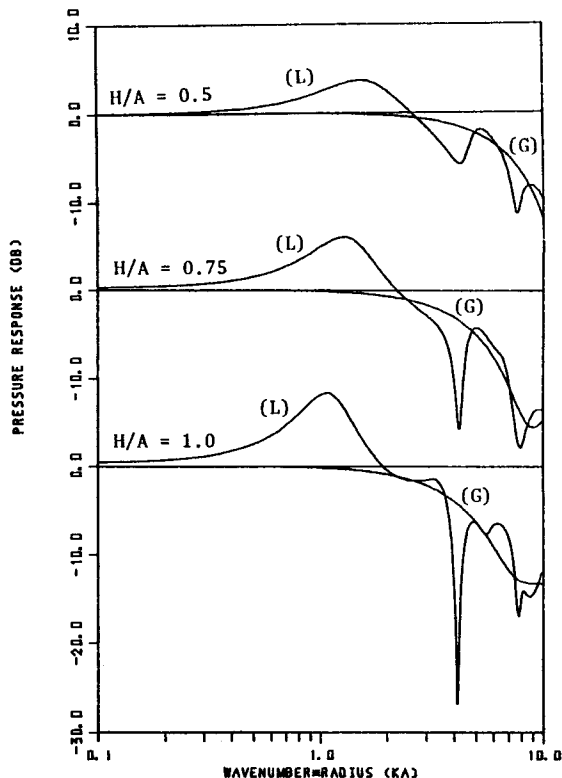


Fig. 5. On-axis pressure responses of a concave dome by the least-square error method (L) and by geometrical approximation (G).

also give a rough estimation of the responses of the concave dome in the high-frequency region. In the middle-frequency region, however, the geometrical approximation is not accurate enough to predict the responses of convex and concave domes.

### 3.1.2 Radiation Impedance

The radiation impedance curves of the convex and concave domes are shown in Figs. 6 and 7, respectively. Fig. 6 also includes the curves for a flat piston. The radiation resistance of the convex dome with  $H/A \geq 0.5$  increases monotonically until about  $kA = 3.0$ . But the rate of increase in this region is smaller than 6 dB/octave. This means that lower radiated power will result in the high-frequency region if the diaphragm is in the inertia control region.

The radiation resistance of the concave dome reaches a maximum, which is much larger than that of the flat piston or the convex dome, at the first resonance of the cavity. This shows that the concave radiator has a much higher efficiency around the high end of the reproducing range of an actual loudspeaker if the diaphragm is rigid in this region.

The radiation reactance of the convex dome is always positive, but the reactance of the concave dome becomes negative above the first cavity resonance.

### 3.1.3 Directivity Pattern

The directivity patterns of the convex and concave domes are shown in Figs. 8 and 9, respectively. At  $kA = 1.0$  the convex dome with  $H/A = 1.0$  shows about a 3-dB lower on-axis sound pressure than the 90-degree off-axis sound pressure, even if the dome vibrates in the axis direction. At  $kA = 2.0$  the directivity pattern of the convex dome shows much larger dispersion of sound than the flat piston. Generally it can be said that

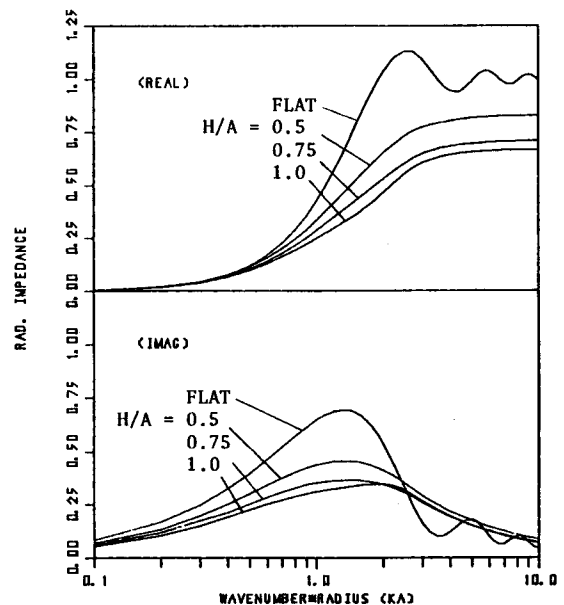


Fig. 6. Radiation impedances of a convex dome and a flat piston normalized by  $\rho c \pi A^2$ .

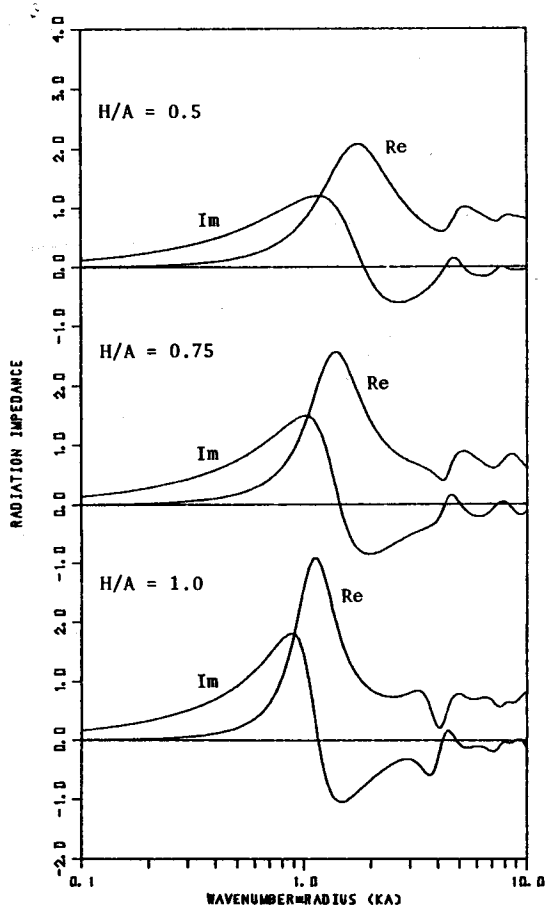


Fig. 7. Radiation impedances of a concave dome normalized by  $\rho c n A^2$ .

the convex radiator has a wider directivity pattern than the flat piston. As Fig. 9 shows, the concave dome and the flat piston have almost the same directivity patterns below  $kA = 3.0$ .

The reason for the lower on-axis pressure response of the convex dome is partly because of the wide dispersion of the radiated power. But the total radiated power still is lower than that of the flat piston or the concave dome radiator, as was discussed in the previous section.

### 3.1.4 Pressure Distribution and Energy Flow

In order to represent the static sound field graphically, contours of the pressure distribution are commonly used. This does not completely describe the sound field because the phase term of the pressure is not shown. The other important quantity which should be shown is the energy flow (or intensity distribution). The benefit of representing the energy flow graphically is that it really shows the details of radiation and diffraction phenomena.

The intensity is defined by

$$I = \frac{1}{2} \text{Re} [p(x) u^*(x)] \quad (17)$$

where \* denotes complex conjugate.

If  $I$  is negative, the energy flows to the negative direction. By computing the  $x$  and  $z$  components of  $I$  first,

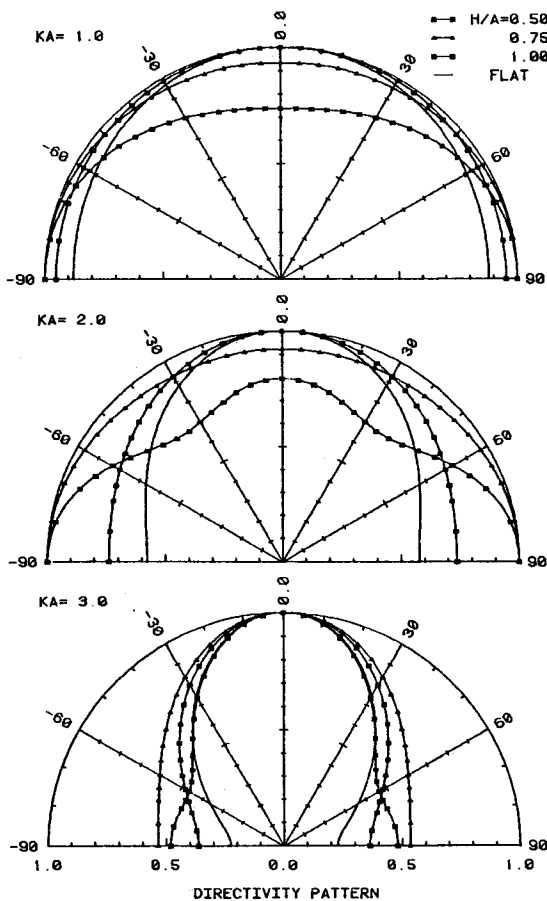


Fig. 8. Directivity patterns of a convex dome and a flat piston.

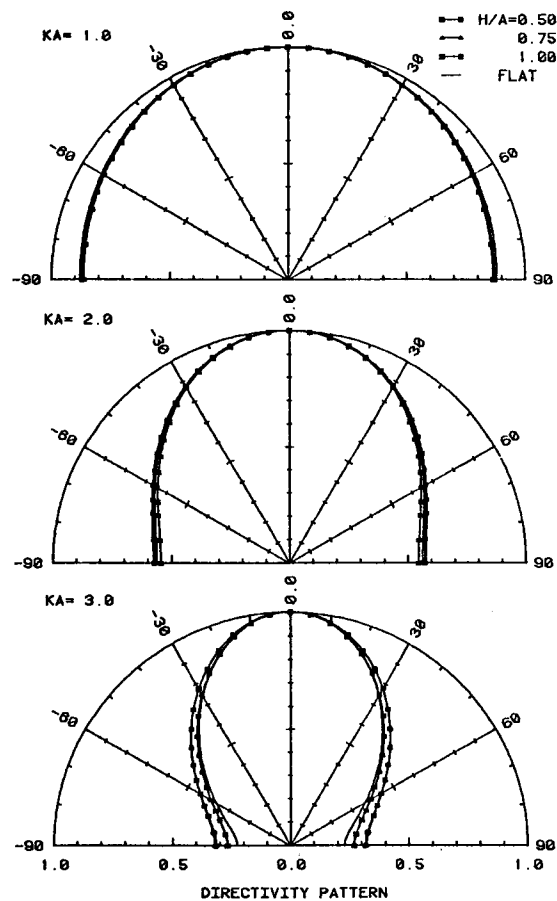


Fig. 9. Directivity patterns of a concave dome and a flat piston.

we can obtain the direction of energy flow and its magnitude. This can be represented graphically by an arrow, the length of which shows the magnitude and the direction of which shows the direction of energy flow.

Figs. 10 and 11 show the energy flow and pressure distribution of the convex and concave domes with  $H/A = 1.0$ . When the frequency is relatively low, the direction of the energy flow on the radiator surface of the convex dome is not normal to it, but is tilted toward the off-axis direction. This results in the lower on-axis pressure response in the far field, as is shown in Fig. 8. As the frequency increases, the power starts to be radiated normal to the surface.

The energy flow inside the cavity of the concave dome is almost parallel to the  $z$  axis if the frequency is below  $kA = 3.0$ . At  $kA = 10.0$ , the energy focuses around the center of the sphere and then spreads into the infinite space.

It is evident that the sound field is visualized more clearly by the energy flow than only by the pressure distribution.

## 3.2 Diffraction by Convex and Concave Dome

### 3.2.1 On-Axis Sound Pressure Response

A ring source with constant acceleration in an infinite baffle has a flat on-axis response if there is no convex or concave object on the baffle. But if one exists on the baffle, the sound field is diffracted by this object. In an actual case the sound emitted by the high-fre-

quency unit of a loudspeaker system will be diffracted by the concave low-frequency unit, resulting in some modification of the response curve of the high-frequency unit. This diffraction phenomenon causes another problem. The high-frequency sound will be amplitude-modulated when the diaphragm of the low-frequency unit makes relatively large excursions. (A point source close to the convex or concave dome is a more suitable model for an actual loudspeaker system. But the ring source will still give us a general idea about the diffraction due to the convex or concave dome.)

Figs. 12 and 13 show the on-axis pressure responses of a concentric ring source with the convex and concave domes, respectively, at the ratio of  $A_1/A = 1.5$ . In Fig. 12, above  $kA = 10.0$ , the differences between the levels of the peaks and dips are more than 10 dB. As the  $H/A$  ratio increases, these differences decrease, and the peaks and dips are shifted to higher frequencies.

As Fig. 13 shows, the existence of the concave dome also affects the on-axis pressure response of the ring source. The effect is smaller than that of the convex dome, except for the first large dip ( $kA = 1.2-1.8$ ). At high frequencies the magnitude of the fluctuation does not depend much on the  $H/A$  ratio and the frequency.

Fig. 14 shows the differences in the responses when the  $H/A$  ratio is changed by  $\pm 0.02$  from  $H/A = 0.5$ . For example, when  $A = 150$  mm, the change in the

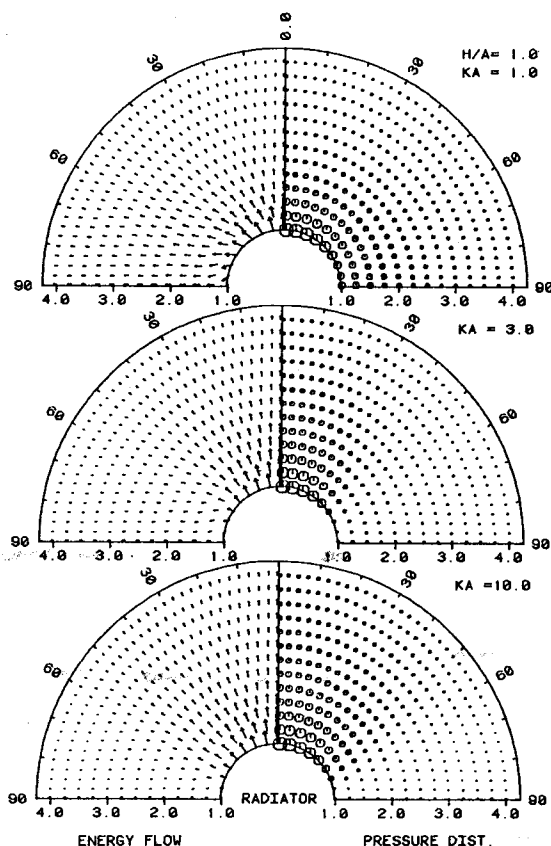


Fig. 10. Pressure distributions and energy flows of a convex dome radiator.

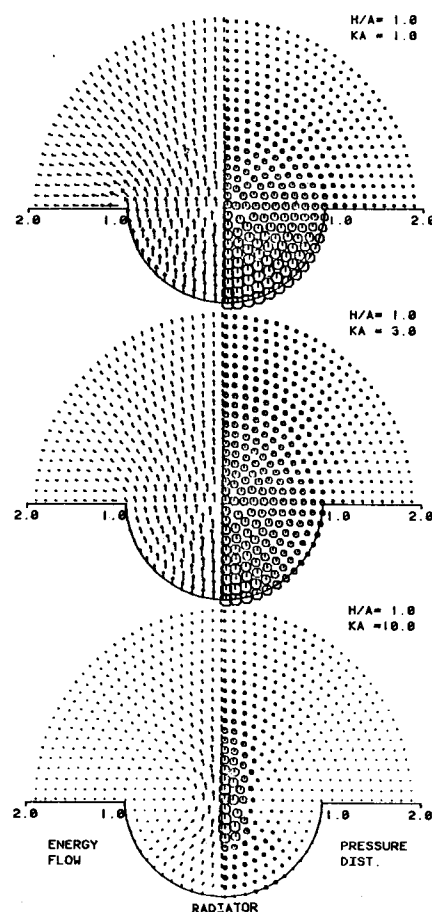


Fig. 11. Pressure distributions and energy flows of a concave dome radiator.

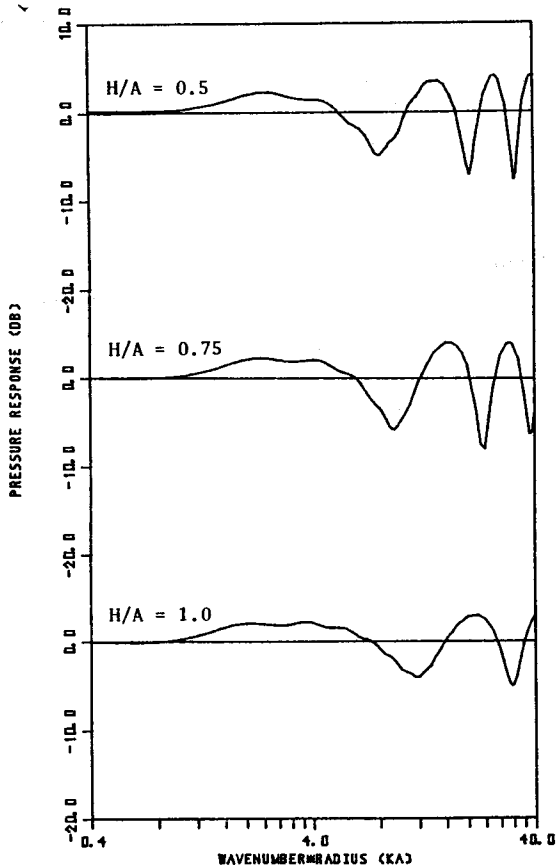


Fig. 12. On-axis pressure responses of a ring source with a concentric convex dome with  $A_1 = 1.5 A$ .

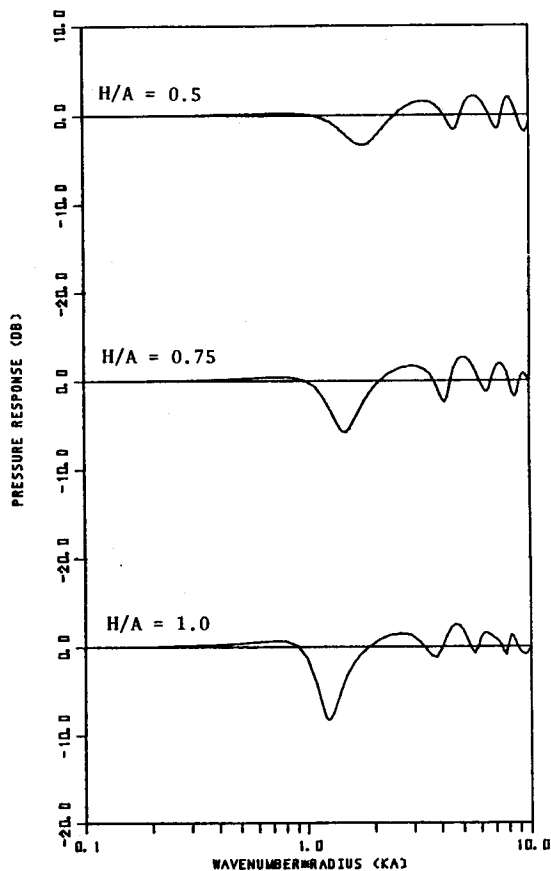


Fig. 13. On-axis pressure responses of a ring source with a concentric concave dome with  $A_1 = 1.5 A$ .

height is  $\pm 3$  mm. Fig. 14 indicates that the change of the height of the dome will produce an amplitude modulation of about  $-30$  to  $-40$  dB at some frequencies.

### 3.2.2 Pressure Distribution and Energy Flow

Figs. 15 and 16 show the pressure distribution and the energy flow of a ring source with convex and concave domes, respectively. Both figures clearly show that the boundary condition of zero normal velocity distribution to the baffle and dome surfaces is satisfied. The convex dome has the property that it diffracts the sound more in the higher frequency region. On the other hand, the concave dome does not have much effect in the high-frequency region. At  $kA = 10.0$  the energy flows along the opening of the cavity. This fact shows that the cavity has a very small effect on the diffraction of the sound. In the middle-frequency region ( $kA = 4.6$ ) the circulation of energy is observed. This may be interpreted as the phenomenon of local standing waves.

## 4 CONCLUSION

The radiation and diffraction effects of convex and concave domes were discussed. The following conclusions can be made:

- 1) The on-axis pressure response changes in a certain extent due to the change of the shape of the diaphragm, even if it vibrates like a piston.
- 2) The radiation resistance shows that the concave dome radiator has much greater efficiency in the high-frequency region of the reproducing range of an actual loudspeaker.
- 3) The convex dome radiator has a wider directivity pattern than the concave radiator in the above-mentioned range.
- 4) The existence of convex and concave domes in an infinite baffle affects the sound pressure response of a sound source located adjacent to them.
- 5) The energy flow as well as the pressure distribution clearly depict the radiation and diffraction effects.

## 5 REFERENCES

[1] S. Ohie, H. Suzuki, and T. Shindo, "Sound Radiation from a Concave Radiator in an Infinite Baffle," *J. Acoust. Soc. Japan*, vol. 34, pp. 429-435 (1978).

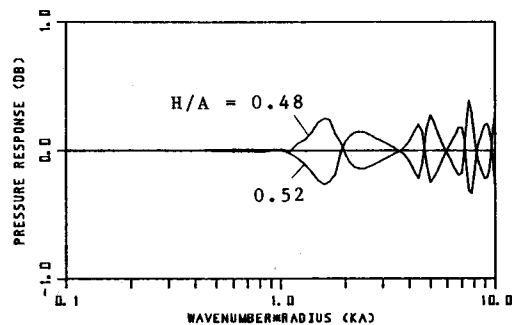


Fig. 14. Changes of the on-axis pressure responses when  $H/A$  is changed by  $\pm 0.02$  from  $H/A = 0.5$ .

[2] T. Shindo, N. Kyono, O. Yashima, T. Yamabuchi, and Y. Kagawa, "The Role of the Dust Cap in the Cone-Type Loudspeaker," presented at the 63rd Convention of the Audio Engineering Society, Los Angeles, 1979 May 15-18.

[3] H. Suzuki and J. Tichy, "Sound Radiation from Convex and Concave Domes in an Infinite Baffle," *J. Acoust. Soc. Am.*, vol. 62, pp. 41-49 (1981 Jan.).

[4] M. Becker, *The Principles and Applications of Variational Method* (M.I.T. Press, Cambridge, MA, 1964).

[5] E. Skudrzyk, *The Foundations of Acoustics* (Springer-Verlag, New York, 1971).

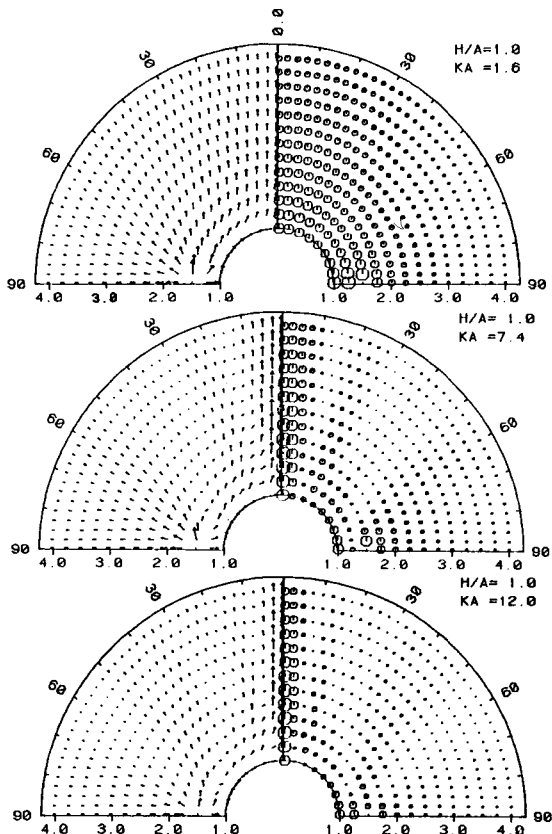


Fig. 15. Pressure distributions and energy flows of a ring source with a concentric convex dome with  $A_1 = 1.5 A$ .

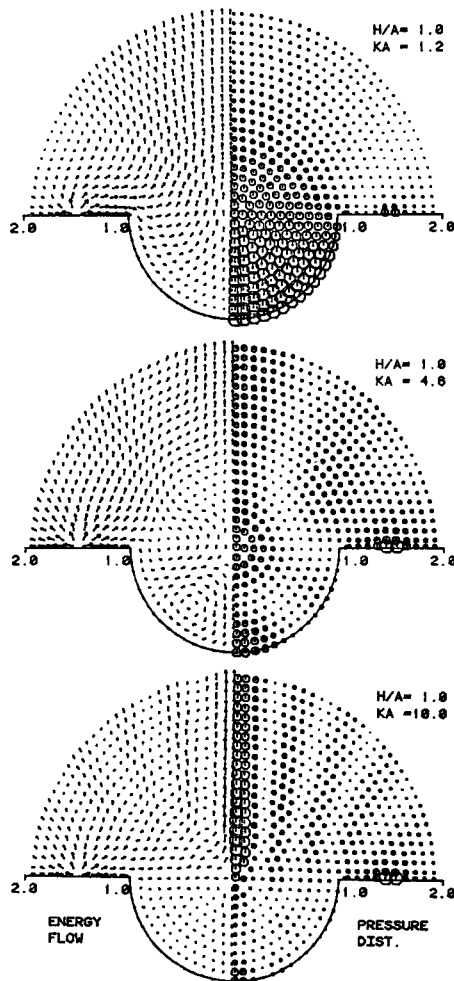


Fig. 16. Pressure distributions and energy flows of a ring source with a concentric concave dome with  $A_1 = 1.5 A$ .

THE AUTHORS



H. Suzuki

Hideo Suzuki has been senior acoustical engineer on the CBS Technology Center staff since mid-1981, following completion of his doctoral program in acoustics at Pennsylvania State University. He had previously studied electrical engineering at Tohoku University, in Japan, obtaining B.S. and M.S. degrees.

In 1967, he joined the Mitsubishi Electric Corpora-



J. Tichy

tion to work in the areas of loudspeaker development. Mitsubishi then sponsored him at Pennsylvania State University in 1972 to study acoustics after which, from 1974 to 1979, he headed the loudspeaker section of the company's Consumer Products Research Laboratory. He returned to Pennsylvania State University, earning his doctorate in 1981. There he